

Environment-governed dynamics in driven quantum systems

S. Gasparinetti,^{1,*} P. Solinas,^{1,2} S. Pugnetti,³ R. Fazio,³ and J. P. Pekola¹

¹*Low Temperature Laboratory (OVLL), Aalto University, P.O. Box 15100, FI-00076 Aalto, Finland*

²*COMP Centre of Excellence, Department of Applied Physics,*

Aalto University School of Science, P.O. Box 11000, 00076 Aalto, Finland

³*NEST, Scuola Normale Superiore and Istituto Nanoscienze-CNR, I-56126 Pisa, Italy*

(Dated: December 14, 2012)

We show that the dynamics of a driven quantum system weakly coupled to the environment can exhibit two distinct regimes. While the relaxation basis is usually determined by the system+drive Hamiltonian (system-governed dynamics), we find that under certain conditions it is determined by specific features of the environment, such as, the form of the coupling operator (environment-governed dynamics). We provide an effective coupling parameter describing the transition between the two regimes and discuss how to observe the transition in a superconducting charge pump.

Introduction. Understanding how quantum systems interact with the environment [1] is of paramount importance in quantum information science. While unveiling how the classical world emerges from the quantum one [2], it can also lead to a better protection against decoherence effects on the way towards the realization of a quantum computer [3].

A standard approach to the dynamics of open quantum systems boils the problem down to the measurement of decoherence rates, distinguishing between coherence loss, or dephasing, and relaxation. While this approach has successfully described a variety of quantum systems, it only offers a limited insight into the dynamics of decoherence. A promising line of work developed in the last decade exploits the possibility of coupling the system to an engineered reservoir [4–12]. The chief advantage of engineered reservoirs is their tunability, allowing one to change at will environment features such as the spectral density, the temperature and the system-environment coupling strength.

As new and more accurate ways are found of harnessing the dynamic evolution of quantum systems, it becomes increasingly important to understand how the interaction with the environment is affected by a time-dependent modulation of the system parameters. Indeed, the study of dissipation in driven quantum systems is a long-established topic [13] that keeps finding new applications, from quantum pumping [14–16] to quantum computation [17, 18].

In this Letter, we consider a periodically driven quantum system in the presence of a weakly coupled environment. We show that under certain conditions decoherence takes place in a preferred basis determined by specific features of the environment, such as, the type of noise, rather than of the system. We label this unusual regime as environment-governed dynamics (EGD), as opposed to the more familiar system-governed dynamics (SGD). We introduce an effective coupling parameter that presides over the transition between SGD and EGD. This parameter can be tuned by changing the properties of the drive. Our analysis is general and applies to opti-

cal and solid-state systems alike. As a relevant example, we propose to observe the transition in a superconducting charge pump [19, 20]. In this system the transition is controlled by an accessible experimental parameter and can be explored by measuring the pumped charge.

Floquet-Born-Markov master equation. We consider a quantum system whose unitary evolution is governed by a periodic Hamiltonian H , so that $H(t) = H(t + \tau)$, where τ is the period. According to Floquet theorem, the Schrödinger equation admits solutions (Floquet states) of the form $|\Psi_\alpha(t)\rangle = e^{-i\epsilon_\alpha t/\hbar} |\varphi_\alpha(t)\rangle$, where the Floquet mode $|\varphi_\alpha(t)\rangle$ satisfies $|\varphi_\alpha(t + \tau)\rangle = |\varphi_\alpha(t)\rangle$ and ϵ_α is its corresponding quasienergy. Quasienergies and their associated modes are defined up to the translation $\epsilon_\alpha \rightarrow \epsilon_\alpha + \hbar\Omega$, where $\Omega = 2\pi/\tau$. As such, all quasienergies can be mapped into the first Brillouin zone $[-\frac{1}{2}\hbar\Omega, \frac{1}{2}\hbar\Omega]$. The Hamiltonian describing the system and its environment is given by $H_{tot} = H(t) + H_E + H_{SE}$, where H_E describes the environmental degrees of freedom and H_{SE} is the interaction term, that we assume of the form $H_{SE} = g S \otimes E$, where g is the adimensional system-environment coupling constant and S and E are operators acting in the Hilbert space of the system and the environment, respectively.

The general procedure for deriving the master equation (ME) in the Floquet basis and in the Born-Markov approximation is outlined in Refs. 13 and 21. The resulting superoperator describing the time evolution of the density matrix is expressed a series of time-independent coefficients multiplied by phase factors of the form $e^{i\Delta_{\alpha,\beta,k} - i\Delta_{\gamma,\delta,k'}}$, with $\Delta_{\alpha,\beta,k} = \epsilon_\alpha - \epsilon_\beta + k\Omega$. Starting from the general expression, we then perform a partial secular approximation (PSA). This amounts to neglecting all terms with $k \neq k'$ while keeping those with $k = k'$ and $\epsilon_\alpha \neq \epsilon_\beta$. A residual time dependence due to terms oscillating like $e^{i(\epsilon_\alpha - \epsilon_\beta)t}$ disappears when passing from the basis of Floquet states to that of Floquet modes. Our result, written in the basis of Floquet modes and in

the Schrödinger picture, reads:

$$\dot{\rho}_{\alpha\beta} = -i(\epsilon_\alpha - \epsilon_\beta)\rho_{\alpha\beta} + \sum_{\gamma,\delta} \rho_{\gamma,\delta} \mathcal{R}_{\alpha,\beta,\gamma,\delta} \quad (1)$$

where

$$\begin{aligned} \mathcal{R}_{\alpha,\beta,\gamma,\delta} = & \Gamma_{\alpha,\gamma,\beta,\delta}^+ + \Gamma_{\alpha,\gamma,\beta,\delta}^- \\ & - \delta_{\delta,\beta} \sum_{\mu} \Gamma_{\mu,\gamma,\mu,\alpha}^+ - \delta_{\gamma,\alpha} \sum_{\mu} \Gamma_{\mu,\beta,\mu,\delta}^- \end{aligned} \quad (2)$$

and

$$\Gamma_{\alpha,\beta,\gamma,\delta}^+ = \sum_k S(\Delta_{\alpha,\beta,k}) X_{\alpha,\beta,k} (X_{\gamma,\delta,k})^* , \quad (3a)$$

$$\Gamma_{\alpha,\beta,\gamma,\delta}^- = \sum_k S(\Delta_{\gamma,\delta,k}) X_{\alpha,\beta,k} (X_{\gamma,\delta,k})^* . \quad (3b)$$

We have introduced the following quantities:

$$S(\omega) = \theta(\omega)J(\omega)n_{\text{th}}(\omega) + \theta(-\omega)J(-\omega)[1 + n_{\text{th}}(-\omega)] ,$$

$$\Delta_{\alpha\beta k} = \epsilon_\alpha - \epsilon_\beta + k\Omega ,$$

$$X_{\alpha\beta k} = \int_0^\tau dt e^{-ik\Omega t} \langle \varphi_\alpha | \hat{B} | \varphi_\beta \rangle ,$$

where $\theta(\omega)$ is the Heaviside function, $J(\omega)$ the spectral density of the bath and $n_{\text{th}}(\omega)$ is the Bose-Einstein distribution.

A few remarks are in order. First, (1) cannot be cast into a Pauli ME [22], i.e., the equations for the diagonal and off-diagonal terms are still coupled. This is due to the fact that we performed a PSA instead of a full secular approximation. The contribution of these terms becomes important close to degeneracies in the Floquet spectrum, where a full secular approximation is expected to fail [23, 24]. The PSA itself is justified provided the drive period is much faster than the decoherence time. This may not be true in the adiabatic limit, where other terms should instead be retained [25].

Equation (1) is formally akin to that of an undriven system, with quasienergies playing the role of ordinary eigenenergies and effective rates given by (3). The presence of a drive manifests itself in the sum over k in (3), allowing the system to exchange energy with the environment in any of the amounts $\Delta_{\alpha,\beta,k}$. The magnitude of this exchange is determined by the noise matrix elements $X_{\alpha,\beta,k}$, telling whether the Floquet modes possess those energies and to what extent the coupling operator S allows the energy transfer to take place. Note that while each individual term in the sums (3) satisfies the detailed balance, the overall rates Γ^\pm in general do not.

Environment-governed dynamics. Equation (1) suggests that the dynamics of the coherences is determined by a competition between two terms. Let us now focus our attention on two states, α and β . For $\alpha \neq \beta$, the first term in (1) is the Floquet energy gap $\mathcal{E} = \epsilon_\alpha - \epsilon_\beta$, stemming from the nondissipative dynamics of the driven

quantum system. The second term describes the effect of dissipation. For sufficiently small values of \mathcal{E} , that is, close to a degeneracy in the Floquet spectrum, the dissipative term can dominate in (1). As a result, the dynamics of states α, β is strongly affected by the environment even if the system and the environment are only weakly coupled, i.e., $g \ll 1$. This is due to the presence of a nearly resonant driving field introducing an energy scale, the Floquet gap, that can be much smaller than those of the undriven system.

Let us now estimate the magnitude of the rates Γ^\pm in (3). We consider an Ohmic environment, whose spectral density is given by $J(\omega) = a\omega f_c(\omega/\omega_c)$, where a is a dimensionless constant, f_c a cutoff function and ω_c the cutoff frequency. In the limit $\Omega \ll \omega_c$ our results are independent of ω_c and the explicit form of f_c . As the sum in (3) runs over k , we may expect the dominant contributions to come from high-frequency modes (large k) such that $X_{\alpha\beta k}$ does not vanish and $k\Omega < \omega_c$. These contributions are of order $g^2(\mathcal{E} + k\Omega) \approx kg^2\Omega$.

We define an effective coupling parameter as

$$\chi = g^2\Omega/\mathcal{E} . \quad (5)$$

If $\chi \ll 1$ we are in the SGD regime. This corresponds to a decoherence time much longer than the period of Rabi oscillations between Floquet modes. By contrast, when $\chi \gtrsim 1$ we enter the EGD regime. This regime is realized close to a (quasi)degeneracy of the Floquet spectrum, where Rabi oscillations between Floquet modes are slower than the decoherence time. We remark that the coupling parameter χ is controlled by the Floquet gap \mathcal{E} , which can be tuned by changing the drive parameters. To appreciate the key role played by the drive, we observe that an undriven system with an arbitrarily small energy gap cannot exhibit EGD. This is due to the fact that for any Ohmic and super-Ohmic environment the transition rates vanish for a vanishing energy gap.

SGD to EGD transition. We will now provide an explicit example of SGD to EGD transition in a driven two-level system. Using a pseudo-spin formalism, we write the system Hamiltonian as $H(t) = \vec{\sigma} \cdot \vec{B}(t)$, where $\vec{\sigma} = \{\sigma_x, \sigma_y, \sigma_z\}$ are the Pauli operators and $\vec{B}(t)$ an effective magnetic field. Specifically, we consider a drive that modulates \vec{B} along the loop shown in Fig. 1(a). This drive is a realization of Landau-Zener-Stückelberg interference [26] with geometric phases [27]. While most of our results are far more general and can be obtained even using a single monochromatic drive, the geometric properties of this particular drive provide a convenient way of tailoring the Floquet spectrum. In the following, we will study the effects of varying the angle φ [see Fig. 1(a)], which naturally controls the solid angle spanned by \vec{B} in pseudo-spin space during a drive period.

In Fig. 1(b) we plot the quasienergy spectrum of the system versus φ . The plot is obtained by numeri-

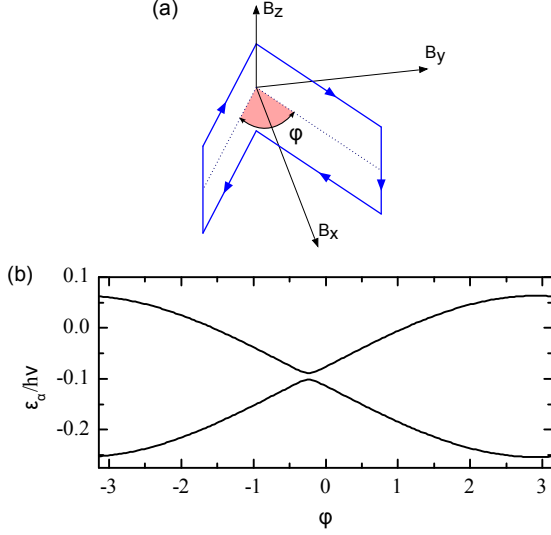


FIG. 1. (Color online) A model driven two-level system. (a) Loop drawn by the effective magnetic field \vec{B} in pseudo-spin space. The solid angle spanned by \vec{B} is controlled by the angle φ . (b) Quasienergy spectrum as a function of φ . A weakly avoided quasienergy crossing occurs at $\varphi_c = -0.26$. The drive parameters are the same as in Fig. 3 with the definitions given in the text.

cally solving the Schrödinger equation for the evolution operator generated by $H(t)$. The quasienergy gap \mathcal{E} sharply decreases near $\varphi = \varphi_c$, where a weakly avoided quasienergy crossing occurs. Close to φ_c , we thus expect EGD to be attained.

We characterize the transition from SGD to EGD by studying the quasistationary state approached by the driven system in the presence of dissipation. For the purpose of illustration, we consider a zero-temperature environment. Our results are obtained by enforcing $\dot{\rho}_{\alpha\beta} = 0$ in (1). This results in a set of algebraic equations for ρ with coefficients $X_{\alpha,\beta,k}$ and \mathcal{E} . Their solution gives the quasistationary density matrix ρ_{st} , which is time-independent in the Floquet-mode basis. We write $\rho_{\text{st}} = 1/2(\mathbb{1} + \vec{n} \cdot \vec{\Sigma})$ where $\vec{\Sigma}$ is the vector of Pauli operators in the Floquet-mode basis. In this way, the residual coherence between Floquet states is associated to the quantity $n_{\perp} = \sqrt{n_x^2 + n_y^2}$.

In Fig. 2(a) we plot n_z (full line) and n_{\perp} (dashed line) versus φ in a neighborhood of φ_c . We choose the noise operator $S = \sigma_z$ and $g^2 = 0.01$. As φ approaches φ_c from either side, we witness the transition from SGD to EGD, signalled by a revival of the coherence between Floquet states.

We then fix φ to a value close to φ_c and change χ by changing g^2 , to which χ is proportional. The results are presented in Fig. 2(b). For small values of g^2 , the coherence between Floquet states is completely lost

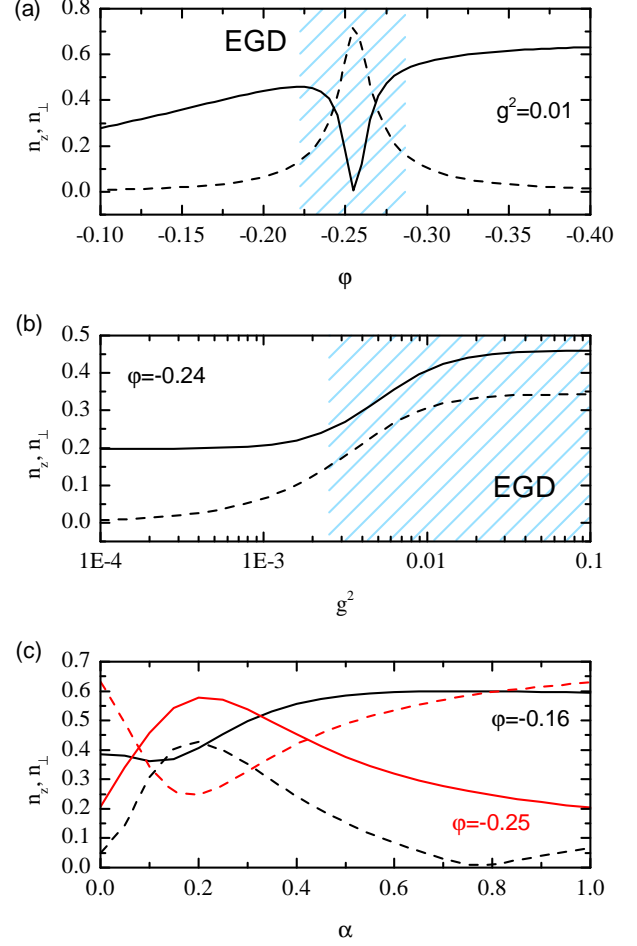


FIG. 2. (Color online) SGD to EGD transition. n_z (full lines) and n_{\perp} (dashed lines) versus φ for $S = \sigma_z$ and $g^2 = 0.01$ (a), versus g^2 for $S = \sigma_z$ and $\varphi = -0.24$ (b), and versus α for $\varphi = -0.16$ (black) and $\varphi = -0.25$ (red) and $g^2 = 0.1$ (c). EGD is attained in the highlighted regions of panels (a,b) and everywhere in panel (c). The drive parameters are the same as in Fig. 3.

($n_{\perp} = 0$, SGD). For larger values of g^2 (but still in the weak-coupling regime), n_{\perp} takes a finite value (EGD). Notice that as soon as either of the two limits is attained, the steady-state populations do not depend on the exact value of g^2 .

A notable feature of the EGD regime is that the preferred basis for relaxation is strongly affected by the type of noise. To demonstrate this, we introduce a family of coupling operators $S(\alpha) = \alpha\sigma_x + (1 - \alpha)\sigma_z$, where $\alpha \in [0, 1]$ parametrizes the angle between the reference basis of H and the noise operator. In Fig. 2(c) we then plot n_z (solid lines) and n_{\perp} (dashed lines) versus α for two different values of φ . We set $g^2 = 0.1$, a value ensuring that the EGD limit is attained for both cases. Upon changing α , ρ_{st} undergoes significant changes. This is in

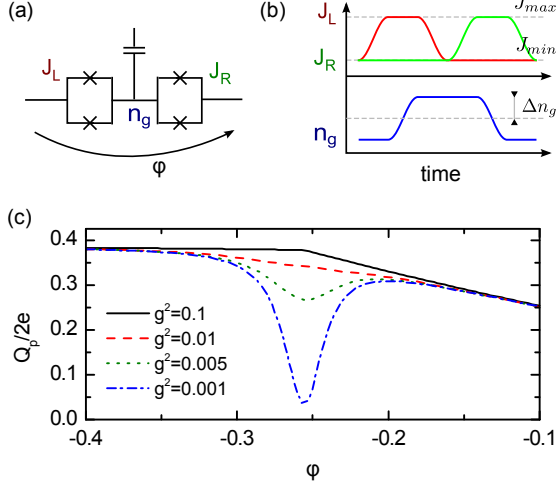


FIG. 3. Application to the Cooper-pair sluice. (a) Equivalent circuit of the sluice. (b) Time dependence of J_L , J_R and n_g during a pumping cycle. (c) Pumped charge Q_p versus φ for selected values of g^2 . The relevant drive parameters [see panel (b)] are: $\tau=1$ ns, $E_C=1$ K, $\Delta n_g = 0.2$, $J_{\max} = 0.1E_C$, $J_{\min} = 10^{-3}J_{\max}$.

stark contrast to what happens in SGD, where relaxation always takes place in the same (Floquet) basis regardless of the coupling operator. Note, however, that even in SGD different coupling operators can result in different populations, as the detailed balance is not satisfied.

As the quasistationary dynamics is determined by a set of algebraic equations, many of these features can be addressed analytically. In the SGD limit ($\chi \ll 1$), we obtain the same results as predicted by a full secular approximation. We find $\rho_{11}^{\text{st}} = \rho_{11,\text{SGD}}$, where $\rho_{11,\text{SGD}}$ is a constant whose explicit expression is found in literature [13, 15], and $\rho_{12}^{\text{st}} = O(\chi)$. By contrast, in the EGD limit ($\chi \gg 1$) we obtain $\rho_{11}^{\text{st}} = \rho_{11,\text{EGD}}$ and $\rho_{12}^{\text{st}} = \rho_{12,\text{EGD}} + O(1/\chi)$. Explicit expressions for the constants $\rho_{11,\text{SGD}}$, $\rho_{11,\text{EGD}}$ and $\rho_{12,\text{EGD}}$ are provided in the Supplemental Material.

Altogether, the results of Fig. 2 show that in the EGD regime the environment is drastically influencing the dynamics of the system. In principle, a steady-state measurement of $n_{x,y,z}$ can thus disclose valuable information on both the type of noise and the strength of system-environment coupling.

Observation in a superconducting charge pump. We now discuss how to observe the SGD to EGD transition in a superconducting charge pump, the Cooper-pair sluice [19, 20, 29]. The sluice, shown schematically in Fig. 3(a), consists of a single superconducting island, coupled to superconducting leads via two superconducting quantum interference devices (SQUIDs). The SQUIDs are operated as Josephson junctions of

tunable energies $J_{L,R}(t)$. A gate electrode capacitively coupled to the island provides a third control parameter by inducing a polarization charge $n_g(t)$ in units of $2e$. The device is operated under a constant superconducting phase bias φ_S . In the charging regime $E_C \gg J_{L,R}$ (E_C is the charging energy of the island), the dynamics can be reduced to the two lowest-energy charge states $|0\rangle$ and $|1\rangle$ corresponding to zero and one excess Cooper pairs on the island, respectively. The system is then described by a pseudospin Hamiltonian of the form discussed above, with effective field components $B_x(t) = \frac{1}{2}J_+(t)\cos\frac{\varphi}{2}$, $B_y(t) = \frac{1}{2}J_-(t)\sin\frac{\varphi}{2}$, and $B_z(t) = E_C[1/2 - n_g(t)]$, where $J_{\pm}(t) = J_L(t) \pm J_R(t)$. Pumping is achieved by steering the three parameters J_L , J_R and n_g in a periodic fashion, as shown in Fig. 3(b).

Starting from the given definitions, it can be shown that the pumping cycle of the sluice is a realization of the loop of Fig. 1(a), with $\varphi = \varphi_S$. The quasienergy gap of the sluice can thus be tuned by changing the superconducting phase bias while performing exactly the same pulse sequence. This makes the sluice an excellent candidate to verify our theoretical predictions.

A further advantage in using the sluice is the possibility to read out the pumped charge Q_p . The formal definition of Q_p , its behavior in the adiabatic limit and its connection with the Berry phase are well understood [30, 31]. In realistic experimental conditions [29, 32], the measured Q_p is often averaged over a great number of cycles. As such, it reflects the quasistationary state reached by the system in the presence of dissipation.

The main source of decoherence in the sluice is charge noise, due to fluctuations in the gate voltage [7, 14]. We describe it by putting $S = \sigma_z$, $\alpha = 1$ and $g = C_g/C_\Sigma$, where C_g and C_Σ are the gate-to-island capacitance and total island capacitance, respectively.

In Fig. 3(c) we plot Q_p as a function of φ for different coupling strengths g^2 . For small values of g^2 , corresponding to $\chi \ll 1$, Q_p exhibits a dip around φ_c . The dip appears in coincidence with the weakly avoided crossing in the quasienergy spectrum [Fig. 1(b)], and stems from the mixing of “adiabatic” Floquet states at the crossing [15, 33]. As g^2 is increased, an expanding neighborhood of φ_c undergoes the transition to EGD, producing an increase in Q_p . Finally, for large enough values of g^2 the whole region of mixing is in the EGD regime, and the dip has disappeared.

Conclusions. A driven quantum system interacting with the environment exhibits a richer scenario than an undriven one. This is due to the emergence of an energy scale, the Floquet gap, that can compete with decoherence rates in the vicinity of a quasienergy crossing. This energy can be tuned by choosing the drive parameters. We have identified two dynamical regimes and given an effective coupling parameter governing the transition between the two. This transition manifests itself in the quasistationary density matrix, in particular, in the re-

vival of coherences between Floquet states. Finally, we have discussed how to observe the transition in a superconducting charge pump. A closely related system that can be considered in a similar spirit is the driven Cooper-pair box [34, 35].

While the SGD regime has been intensively studied, the EGD regime is vastly unexplored. Due to its simplicity and applicability to a variety of different systems, the present approach may emerge as a useful tool to study system-environment interactions in open quantum systems.

Acknowledgements. We would like to thank J. Ankerhold, C. Ciuti, V. Gramich, M. Möttönen, J. Salmilehto and M. Silveri for useful discussions. This work was supported by the Finnish National Graduate School in Nanoscience, by the European Community's Seventh Framework Programme under Grant Agreement No. 238345 "GEOMDISS", and partially by the Academy of Finland through its Centres of Excellence Program (project No. 251748). P.S. acknowledges financial support from FIRB – Futuro in Ricerca 2012 under Grant No. RBFR1236VV "HybridNanoDev".

* simone.gasparinetti@aalto.fi

- [1] H. P. Breuer and F. Petruccione, *The Theory of Open Quantum Systems* (Oxford University Press, 2007).
- [2] W. H. Zurek, *Rev. Mod. Phys.* **75**, 715 (2003).
- [3] M. A. Nielsen and I. L. Chuang, *Quantum Computation and Quantum Information* (Cambridge University Press, 2000).
- [4] C. Myatt, B. King, Q. Turchette, C. Sackett, D. Kielpinski, W. Itano, C. Monroe, and D. Wineland, *Nature* **403**, 269 (2000).
- [5] D. Kielpinski, V. Meyer, M. A. Rowe, C. A. Sackett, W. M. Itano, C. Monroe, and D. J. Wineland, *Science* **291**, 1013 (2001).
- [6] H. Weimer, M. Müller, I. Lesanovsky, P. Zoller, and H. P. Büchler, *Nat. Phys.* **6**, 382 (2010).
- [7] P. Solinas, M. Möttönen, J. Salmilehto, and J. P. Pekola, *Phys. Rev. B* **82**, 134517 (2010).
- [8] J. T. Barreiro, M. Müller, P. Schindler, D. Nigg, T. Monz, M. Chwalla, M. Hennrich, C. F. Roos, P. Zoller, and R. Blatt, *Nature* **470**, 486 (2011).
- [9] S. Diehl, E. Rico, M. a. Baranov, and P. Zoller, *Nat. Phys.* **7**, 971 (2011).
- [10] B.-H. Liu, L. Li, Y.-F. Huang, C.-F. Li, G.-C. Guo, E.-M. Laine, H.-P. Breuer, and J. Piilo, *Nat. Phys.* **7**, 931 (2011).
- [11] P. Solinas, M. Möttönen, J. Salmilehto, and J. P. Pekola, *Phys. Rev. B* **85**, 024527 (2012).
- [12] K. W. Murch, U. Vool, D. Zhou, S. J. Weber, S. M. Girvin, and I. Siddiqi, *Phys. Rev. Lett.* **109**, 183602 (2012).
- [13] M. Grifoni and P. Hänggi, *Phys. Rep.* **304**, 229 (1998).
- [14] J. P. Pekola, V. Brosco, M. Möttönen, P. Solinas, and A. Shnirman, *Phys. Rev. Lett.* **105**, 030401 (2010).
- [15] A. Russomanno, S. Pugnetti, V. Brosco, and R. Fazio, *Phys. Rev. B* **83**, 214508 (2011).
- [16] F. Pellegrini, C. Negri, F. Pistolesi, N. Manini, G. E. Santoro, and E. Tosatti, *Phys. Rev. Lett.* **107**, 060401 (2011).
- [17] S. Diehl, A. Micheli, A. Kantian, B. Kraus, H. P. Büchler, and P. Zoller, *Nat. Phys.* **4**, 878 (2008).
- [18] A. Ferrón, D. Domínguez, and M. J. Sánchez, *Phys. Rev. Lett.* **109**, 237005 (2012).
- [19] A. O. Niskanen, J. P. Pekola, and H. Seppä, *Phys. Rev. Lett.* **91**, 177003 (2003).
- [20] A. O. Niskanen, J. M. Kivioja, H. Seppä, and J. P. Pekola, *Phys. Rev. B* **71**, 012513 (2005).
- [21] R. Blümel, A. Buchleitner, R. Graham, L. Sirko, U. Smilansky, and H. Walther, *Phys. Rev. A* **44**, 4521 (1991).
- [22] K. Blum, *Density Matrix Theory and Applications* (Springer, 2012), 2nd ed.
- [23] T. Dittrich, B. Oelschlägel, and P. Hänggi, *Europhys. Lett.* **22**, 5 (1993).
- [24] B. Oelschlägel, T. Dittrich, and P. Hänggi, *Acta Phys. Pol. B* **24**, 845 (1993).
- [25] I. Kamleitner and A. Shnirman, *Phys. Rev. B* **84**, 235140 (2011).
- [26] S. N. Shevchenko, S. Ashhab, and F. Nori, *Phys. Rep.* **492**, 1 (2010).
- [27] S. Gasparinetti, P. Solinas, and J. P. Pekola, *Phys. Rev. Lett.* **107**, 207002 (2011).
- [28] See Supplemental Material.
- [29] M. Möttönen, J. J. Vartiainen, and J. P. Pekola, *Phys. Rev. Lett.* **100**, 177201 (2008).
- [30] J. P. Pekola, J. J. Toppari, M. Aunola, M. T. Savolainen, and D. V. Averin, *Phys. Rev. B* **60**, R9931 (1999).
- [31] M. Aunola and J. J. Toppari, *Phys. Rev. B* **68**, 020502(R) (2003).
- [32] S. Gasparinetti, P. Solinas, Y. Yoon, and J. P. Pekola, *Phys. Rev. B* **86**, 060502(R) (2012), 1206.0193.
- [33] D. W. Hone, R. Ketzmerick, and W. Kohn, *Phys. Rev. E* **79**, 051129 (2009).
- [34] C. M. Wilson, T. Duty, F. Persson, M. Sandberg, G. Johansson, and P. Delsing, *Phys. Rev. Lett.* **98**, 257003 (2007).
- [35] C. M. Wilson, G. Johansson, T. Duty, F. Persson, M. Sandberg, and P. Delsing, *Phys. Rev. B* **81**, 024520 (2010).

Quasistationary solution for the master equation

Starting from Eq. (1) in the main text, we restrict ourselves to a two-level system and set $\dot{\rho}_{\alpha\beta} = 0$. We are not here interested in the details of the solution but only in its scaling with respect to the quantities g , Ω and \mathcal{E} .

We represent the quasistationary solution ρ_{st} as a vector of components $(\rho_{11}^{\text{st}}, \rho_{12}^{\text{st}}, \rho_{21}^{\text{st}}, \rho_{22}^{\text{st}})$. Using (1), the definitions (2) and (3) and the symmetries of the rates (3), we find that $\vec{\rho}_{\text{st}}$ satisfies the following matrix equation:

$$\left[g^2 \Omega \begin{pmatrix} m & n & n^* & o \\ p & q & r & s \\ p^* & r^* & q & s^* \\ -m & -n & -n^* & -o \end{pmatrix} - i\mathcal{E} \begin{pmatrix} 0 & 0 & 0 & 0 \\ 0 & 1 & 0 & 0 \\ 0 & 0 & -1 & 0 \\ 0 & 0 & 0 & 0 \end{pmatrix} \right] \cdot \vec{\rho}_{\text{st}} = 0 . \quad (6)$$

where m, \dots, s are a set of dimensionless coefficients. We have factored out a factor $g^2 \Omega$ in the Redfield tensor (2) as this is its expected scaling in the case we consider (Ohmic environment, $\Omega \ll \omega_c$).

For simplicity, let us assume that all coefficients in (6) are real (it turns out that this is often the case). The exact solution is then given by:

$$\rho_{11}^{\text{st}} = \frac{A}{C}, \rho_{12}^{\text{st}} = \frac{D}{C}, \quad (7)$$

with

$$\begin{aligned} A &= (q - r)[o(q + r) - 2ns]g^4\Omega^2 + o\mathcal{E}^2, \\ C &= 2n(q - r)(p - s)g^4\Omega^2 - (m - o)[(q^2 - r^2)g^4\Omega^2 + \mathcal{E}^2], \\ D &= (ms - op)[(q - r)g^2\Omega + i\mathcal{E}]g^2\Omega. \end{aligned}$$

In the SGD regime $\chi \ll 1$, $A \approx o\mathcal{E}^2$, $C \approx (o - m)\mathcal{E}^2$ and $D \approx i(ms - op)g^2\Omega\mathcal{E}$. An approximate solution is

$$\rho_{11}^{\text{st}} = \frac{o}{o - m} \equiv \rho_{11, \text{SGD}}, \quad (8a)$$

$$\rho_{12}^{\text{st}} = i \frac{op - ms}{m - o} \frac{g^2\Omega}{\mathcal{E}} = \mathcal{O}(\chi), \quad (8b)$$

The coherence ρ_{12}^{st} vanishes for infinitesimally weak coupling, indicating that the Floquet basis is the relaxation basis. Furthermore, (8a) does not depend on the coupling strength. These results are the same as obtained with a full secular approximation [13, 15].

In the EGD regime $\chi \gtrsim 1$, an approximate solution is:

$$\rho_{11}^{\text{st}} = \frac{o(q + r) - 2ns}{2n(p - s) - (m - o)(q + r)} \equiv \rho_{11, \text{EGD}}, \quad (9a)$$

$$\rho_{12}^{\text{st}} = \frac{ms - op}{2n(p - s) - (m - o)(q + r)} \left(1 + \frac{i}{q - r} \frac{\mathcal{E}}{g^2\Omega} \right) \equiv \rho_{12, \text{EGD}} + \mathcal{O}\left(\frac{1}{\chi}\right). \quad (9b)$$

The coherence ρ_{12}^{st} in general does not vanish; in the limit $\chi \gg 1$, it also approaches a constant value.